Desalination and Water Treatment
www.deswater.com

doi: 10.5004/dwt.2023.29215

283 (2023) 209–221
January

Heterogeneous activation of peroxide via acid-modified red mud for the degradation of phenol

Hongliang Chen[a,b,*], Qian Long[b], Fuhua Wei[a,b]

[a]*College of Chemistry and Chemical Engineering, Anshun University, 25 Xueyuan Road, Xixiu District, Anshun, Guizhou Province 561000, China, Tel.: +86-0851-32214860; Fax: +86-0851-32214860; emails: chenhledu@126.com (H. Chen), qingquan000000@163.com (F. Wei)*
[b]*Chemical Process Centre for comprehensive treatment of industrial solid waste, Anshun University, Anshun, Guizhou 561000, China, Tel.: +86-0851-32214860; Fax: +86-0851-32214860; email: 759980003@qq.com*

Received 7 June 2022; Accepted 9 December 2022

ABSTRACT

The pollution of phenolic wastewater has aroused the growing attention. Developing an efficient and inexpensive catalyst to degrade phenol is critical to the wastewater purification technology. Thus, a novel acid-modified red mud catalyst (RM4) containing abundant functional groups and pore structures was prepared. The characteristics of catalysts were determined by the X-ray diffractometer, the scanning electron microscopy and the X-ray photoelectron spectroscopy. α-Fe_2O_3 and β-Fe_2O_3 in RM4 played the crucial roles in the peroxide (H_2O_2) activation for the degradation of phenol. The removal efficiency of phenol was 96.8% under the optimization conditions of 0.02 M of H_2O_2, 50 mL of 100 mg/L phenol, 0.05 g of RM4 and reaction time 120 min. The degradation of phenol fit into the pseudo-first-order kinetics model with the control of the inherent chemical reaction. The removal efficiency of phenol (96.8%) was inconsistent with the removal efficiency of chemical oxygen demand (88.2%), signifying that carboxylic intermediates probably accumulated in the degradation process. Mechanism analysis indicated that •OH was the predominant radical and gave the possible degradation pathways. Continuous experiments were carried out as the preliminary step of future pilot scale tests. This study proposed that RM4 was a low cost, easily prepared and environmental catalyst as H_2O_2 activator for the phenol degradation in water.

Keywords: Acid-modified red mud; Peroxide; Heterogeneous activation; Degradation of phenol; Continuous experiments

1. Introduction

Phenol and its derivative chemicals are a group of highly resistant aromatic chemical compounds of difficult decomposition in the environment. Phenol is essential in the synthesis processes of pharmaceuticals, herbicides, detergents, plastics, flame retardants, epoxies, nylon and other fine chemicals [1], and phenolic compounds are main pollutants in petrochemical and coal processing [2]. Phenol is corrosive to eyes, skin and the respiratory tract, causing dermatitis. Long-term exposure may be associated to health conditions affecting the central nervous system, heart, liver and kidneys [3]. Phenolic compounds are suspected carcinogenic compounds. In the meantime, phenol is identified as one of the top priority pollutants due to its ecotoxicological effects. The methods of phenolic compounds treatment mainly includes electrocatalytic degradation [2], filtration [4], adsorption [5], biological treatment

* Corresponding author.

[6,7], advanced oxidation processes (AOPs), etc. However, many limitations have been reported for above-mentioned methods. Complex and expensive designs of electrochemical reactors, high mass transfer limitation, high energy consumption and difficult maintenance are some of the disadvantages of conventional electrocatalytic degradation systems. For filtration, lack of sufficient effectiveness in eliminating contaminants with high molecular weights, detecting membrane clogging, and need for careful maintenance of membranes are considered as the limitations. For the adsorption, low efficiency at high concentration of pollutants and need for regeneration of the adsorbent have been reported for the adsorption techniques. Inhibitory effect on the biological activity of microorganisms responsible for wastewater degradation in the presence of high concentration of pollutants has been identified as the limitation of the biological treatment. AOPs have been used as an effective option for the wastewater treatment and are promising systems based on hydroxyl radicals (•OH) with the higher oxidative potential (2.8 V) for the chemical oxidation of organic contaminants in volatile organic compounds, groundwater and bitumen post-oxidative effluents compared with ozone (E_0 = 2.0 V) or H_2O_2 (E_0 = 1.80 V) [8,9]. Fenton-like oxidation, a type of AOPs, has been proven as the technology with advantages of nonselective oxidation, no secondary pollution and eco-friendliness in the degradation of phenol, and attracts widespread research interests for the practical wastewater treatment. In homogeneous Fenton process, the generation of ferric hydroxide sludge is regarded as a secondary pollution and limits its large-scale application [10]. To minimize negative effects and overcome the drawbacks of homogeneous Fenton process, heterogeneous Fenton-like processes receive more and more attentions due to its easy separation [9]. This results in the development of heterogeneous process. Various metal oxides (such as Fe_2O_3, MnO_2, ZnO, Al_2O_3, ZrO_2, SiO_2, TiO_2, etc.) have been reported as suitable catalysts for the oxidation of phenol [8,10,11]. However, the employment of these metal oxides faces an economic issue regarding scaling up. Therefore, it is of great significance to develop heterogeneous Fenton-like catalysts with high activity and low-cost.

Industrial solid wastes, including steel slag, tailings, fly ash, red mud, electrolytic manganese residue, waste tires, rubber, etc, have become the most serious concerns fronting society due to a significant amount of stock, masses of heavy metals and other harmful substances [12,13]. Stockpiling of these industrial solid wastes occupies a large amount of land resources and seriously affects the ecological environment. The industrial solid wastes contain metal-contained oxides, porous structure and high specific surface area, which can offer a large number of active sites for the catalytic reaction, reduce the possibility of deactivation, and increase the service life of the catalyst [14–17]. These wastes have attracted wide attentions for the degradation of refractory organics from wastewater in the light of easy acquisition, low cost and the strategy of "treat waste by waste". Nasuha et al. [15] investigated the degradation performance of methylene blue and acid blue 29 dyes by electric arc furnace steel slag activated via sulfuric acid under the dark-Fenton process conditions, and discovered that the degradation of the dyes realized 95% and 82%, respectively. Xu et al. [16] reported that the efficient degradation of Rhodamine B by bimetallic CoMn oxides loaded on coal fly ash-derived SBA-15 activating peroxymonosulfate, and found the dominant reactive oxygen species was $^1O_2$. Lan et al. [14] discovered that 99% of azo dyes were degraded in the Fenton-like process by the modified electrolytic manganese residue with a nanosheet structure. Based on the review of literatures, before the catalysis degradation of refractory organics, the structures and properties of industrial solid wastes need adjusting and modifying by metal-doping, metal oxides loading, ultrasonic etching, pyrolysis or acid activation to enhance the catalytic capacity and releasing more active sites [12,13]. Red mud (RM) is a solid waste generated during the bauxite refining of alumina. Bayer process discharges 0.8–1.5 tons of RM for producing per ton of alumina [18]. About 120 million tons of RM is produced around the world, of which China produces about 30 million tons per year [19]. Various applications of RM in environmental fields have been reported. There are three general categories for the environmental remediation materials: including waste water purification, waste gas purification and soil remediation [20,21]. In addition, modified RM has been used in the bio-oil preparation from the corn stover [18,22], biomass gasification tar cracking [18], adsorption of inorganic anions and organic pollutants [20], etc. There are plenty of SiO_2, Al_2O_3, CaO, Fe_2O_3, TiO_2, and a small quantity of MnO, ZrO_2, SrO, NiO, NbO, etc in red mud [23]. These compounds are advantageous for the application during the degradation of refractory organics from wastewater, while realizing the utilization of waste products. Recently, some studies have been reported using RM as catalysts, such as the preparation of a new Fenton-like catalyst for the degradation of sulfamethoxazole, and co-carbonization of red mud and waste sawdust as a Fenton catalyst for Rhodamine B oxidation [24,25]. Thus, RM could serve as an inexpensive and sacrificial catalyst that could be effectively applied to the phenol degradation. Nevertheless, raw RM has limited functional groups and underdeveloped pore structures. Thus, efforts are ongoing to enhance the catalytic performance of RM, and the use of various acids, such as HCl, HNO_3 and H_2SO_4, induced an increase in the number of functional groups under appropriate conditions [15,26].

In this study, RM was used as the targeted feedstock to produce the catalysts. The physicochemical characteristics were systematically determined during the process of acid modifying RM. The catalytic capacity of the modified RM was determined in batch and continuous experiments by using phenol as a model pollutant. The effect of inorganic anions on the degradation of phenol, leaching of metal ions, the change of chemical oxygen demand (COD) during the degradation of phenol and the reusability of catalysts were examined. The phenol degradation fitting into the kinetics model was investigated. To identify highly active radicals (HARs) and suggest a catalytic mechanism for the catalyst of the best catalytic performance, quenching experiments and the electron spin resonance (ESR) experiments were conducted. Continuous experiments were carried out as the preliminary step of future pilot scale tests. Research novelty was the application of RM waste to the degradation of refractory organics via the simple processing.

2. Materials and methods

2.1. Materials and chemicals

Red mud was collected from an alumina refinery plant in Anshun City, Guizhou Province, China, and mainly contained 19.78% SiO_2, 19.78% Al_2O_3, 18.8% CaO, 11.09% Fe_2O_3, 7.0% Na_2O, 6.5% TiO_2, 2.49% SO_3, 1.85% K_2O and 0.2% MnO, etc by an X-ray fluorescence (XRF) spectrometer (XRF-1800, Shimadzu, Japan) analysis. Phenol (C_6H_6O), hydrochloric acid (HCl), ammonia solution (NH_3), peroxide (H_2O_2), methanol (CH_4O) and *tert*-butanol ($C_4H_{10}O$) were purchased from Shanghai Macklin Biochemical Co., Ltd., China. Ferric sesquioxide (Fe_2O_3) was obtained from Guangdong Guanghua Sci-Tech Co., Ltd., China. All used chemicals were without further purification.

2.2. Preparation of catalysts

Red mud was washed with deionized water until a constant pH. Subsequently, the mixture was vacuum-filtrated. The obtained sample was dried in an oven and marked as WRM. 50 g of WRM was added to a 1 L beaker (Shuniu, China) with 500 mL of 2 M HCl and brought to the boil on an electric furnace (DN-DL-1, SUNNE, China) for 30 min. After cooling, the mixture stood at room temperature for 24 h and ammonia solution was added into the mixture to adjust pH to 3.0, 4.0, 5.0 and 6.0, respectively. These mixtures were vacuum-filtrated and the filtered solids were dried about 6 h in an oven at 105°C for tests. The obtained filtered solids under pH = 3.0, 4.0, 5.0 and 6.0 were marked as RM3, RM4, RM5 and RM6, respectively. Modified Fe_2O_3 (MFO) as a comparison was also prepared by the same method as RM4 preparation using commercial Fe_2O_3 (FO). Active components (Fe_2O_3, MnO_2, etc.) were dissolved out from the intra particle of RM by HCl under boiling. Ammonia solution was added into the mixture to adjust expectant pH in order to uniformly precipitate active components on the surface of RM.

2.2.1. Characterizations of catalysts

Phase compositions of modified red mud samples were characterized by an X-ray diffractometer (XRD) (X'Pert PRO, PANalytical, Holland). Images and components of the samples were recorded by a scanning electron microscopy (MIRA4-LMH, TESCAN, Czech Republic) equipped with an energy-dispersive X-ray spectroscopy (EDS) (One Max 50, Oxford, UK). Surface elemental compositions and valence status of samples were further analysed using an X-ray photoelectron spectroscopy apparatus (XPS) (ESCALAB 250XI, Thermo, USA). HARs were monitored by an electron spin resonance spectroscopy (ESR) (A300, BRUKER, Germany).

2.3. Reaction procedures

In phenol degradation processes, a temperature-controlled shaker (SHZ-82A, Sanpu, China) was used at 100 rpm. For batch experiments, 50 mL of 100 mg/L phenol was placed into a 250 mL conical flask (Shuniu, China), after which 0.05 g catalyst and a certain concentration of H_2O_2 were added into the conical flask. Once H_2O_2 was added into the phenol solution, the degradation reaction was triggered. Three runs of each trial were conducted, and the average values and error bars were reported. During phenol degradation, the catalytic performance of different samples and influencing factors, such as H_2O_2 concentration, initial concentration of phenol, initial pH and catalyst dosage, were investigated. The catalytic performance of different samples on the phenol degradation were conducted under 0.05 g of catalyst, 0.02 M H_2O_2, 100 mg/L of phenol within 120 min at room temperature (25°C ± 1°C). The influences of H_2O_2 concentration, initial concentration of phenol, initial pH and catalyst dosage were as follows: the effect of H_2O_2 concentration (0–0.1 M) was investigated with 0.05 g of catalyst, 50 mL of 100 mg/L phenol, initial pH 5.6 and 120 min of reaction time for RM4; The effect of initial concentration (50–200 mg/L) of phenol was explored under 0.05 g of catalyst, 0.02 M H_2O_2, initial pH 5.6 and 120 min of reaction time for RM4; When the experiment conditions were 0.05g of catalyst, 50 mL of 100 mg/L phenol, 0.02 M H_2O_2 and 120 min of reaction time, the effect of initial pH 3–8 on the degradation of phenol was probed using RM4; The effect of added catalyst dosage (0.01–0.1 g) was surveyed with 0.02 M H_2O_2 concentration, initial pH 5.6 and 120 min of reaction time. The degradation of phenol fitting into the kinetics model was investigated at 25°C–50°C via 100 and 150 mg/L of phenol. Intermediates of phenol degradation were identified by a liquid chromatograph–mass spectrometer (LCMS) (Agilent 1100-AB 400, USA). Quenching experiments were conducted to confirm HARs in catalyst/H_2O_2 system during the phenol degradation using methanol and *tert*-butanol. HARs were also monitored by ESR experiments via the formation of DMPO-OH adduct. Continuous experiments were carried out in a self-made device using the uppermost performance catalyst with 50, 100 and 200 mg/L phenol, respectively. The removal efficiency of phenol were measured with definite concentration of phenol under different flows (0.2–2.5 mL/min). After expected time, the solution samples were taken out and then measured after being filtered with a 0.45-mm membrane. The concentration of phenol was measured by an Agilent1260 HPLC using a UV detector set at 280 nm and the mobile phase was a mixture of 40% CH_3CN and 60% ultrapure water.

The phenol removal efficiency (ϕ) is calculated using Eq. (1):

$$\varphi(\%) = 100\frac{(C_0 - C)}{C_0} \tag{1}$$

where C_0 (mg/L) and C (mg/L) are the initial and time-dependent concentration of phenol, respectively.

3. Results and discussion

3.1. Material characterization

Phase compositions of acid-modified red mud were characterized by XRD technology, which is shown in Fig. 1. The XRD patterns of RM4 and RM5 (Fig. 1a) were similar and manifested the existence of a-Fe_2O_3, b-Fe_2O_3, $Al(OH)_3$, MnO_2, Ca_2SiO_4, $NiTiO_3$ and $CaTiO_3$. a-Fe_2O_3, b-Fe_2O_3 and

Table 1
Comparison of relevant studies of phenol degradation

Removal efficiency of phenol	Catalysts	Oxidisers	Experiment conditions	References
96.8%	RM4	H_2O_2	0.02 M of H_2O_2; 100 mg/L of phenol; 0.05 g RM4; 120 min at 25°C	This paper
90%	Dendritic Fe^0	H_2O_2	50 mg/L phenol; 6 mmol/L H_2O_2; 0.1 g/L catalyst; 16 min	[8]
80.6%	$Fe_{0.7}Zn_{0.3}S$	H_2O_2	0.2 mmol/L phenol; initial pH = 3.5; 3.0 mmol/L H_2O_2; 0.1 g/L catalyst; 2 min; ambient temperature	[10]
97.6%	γ-Fe_2O_3/MnO_2	Peroxymonosulfate	35 mg/L phenol; 0.5 g/L PMS; 0.3 g/L catalyst; pH 6.4; 30°C	[11]
100%	Co/RM	Oxone	30 ppm phenol; 0.4 g/L; catalyst 2 g/L oxone; 25°C; 90 min	[34]

$Al(OH)_3$ in RM4 and RM5 were probably from the conversion of $Ca_3Al_2(SiO_4)(OH)_8$, $Ca_3AlFe(SiO_4)(OH)_8$ and $Na_8(AlSiO_4)_6(CO_3)(H_2O)_2$ in WRM under acidic conditions. Fig. 1b showed that a part of a-Fe_2O_3 from commercial FO was translated into b-Fe_2O_3 under the same conditions as RM4 was prepared, which supported the formation of b-Fe_2O_3 in RM4 and RM5. Habibi et al. [27] discovered that hematite, chamosite and poorly crystalline goethite presented in the red mud matrix were converted into Fe_2O_3 under acidic conditions. a-Fe_2O_3, b-Fe_2O_3 and MnO_2 were probably main compositions of activator for oxidants removing phenol [11], and had a stronger characteristic peak in RM4 compared with RM5. Zhang et al. [28] employed cubic b-Fe_2O_3 as an excellent catalyst for photo-Fenton degradation of Rhodamine B and phenol, and acquired the higher degradation removal rates. Like bread peak of RM3 indicated the formation of amorphous structure of some a-Fe_2O_3 and $Al(OH)_3$ during preparing RM3, which probably brought about an insufficient catalytic performance for phenol degradation. The characteristic XRD peaks of $Ca_3Al_2(SiO_4)(OH)_8$, $Ca_3AlFe(SiO_4)(OH)_8$, MnO_2, Ca_2SiO_4, $NiTiO_3$, $CaTiO_3$, Fe_2O_3 and $Al(OH)_3$ were identified in RM6, suggesting that a mass of substances similar to the compositions of WRM formed when the pH was increased to 6.

Morphology and microstructure of WRM, RM3, RM4, RM5, RM6 and MFO were examined by scanning electron microscopy (SEM). The images for the studied samples are presented in Fig. 2. WRM had rough and uneven particles, and consisted of a submicron size with globular structures. Fig. 2b–e show that there were highly porous particles in smaller diameter compared with WRM after RM was treated using HCl. By comparison among RM3, RM4, RM5 and RM6, RM4 had the smallest particle diameter and bore diameter of apertures (Fig. 2c–c_1), and formed advantageously an even distribution of Fe_2O_3, as shown in Fig. 2c_2. It was reported that the distribution of Fe_2O_3, smallest particles and more apertures, supported and raised the catalytic performance of materials [8,11]. The surface particles of MFO (shown in Fig. 2f) had the smaller diameter compared with WRM.

Surface elemental composition and valence status of WRM and RM4 were characterized by XPS spectra. The total XPS survey spectrum in Fig. 3a reveals that Fe, Mn, O, C, etc existed on the surface of RM4. Fe had the higher content on the surface of RM4 compared with Mn. There was an encouraging sign that the low content of Mn formed on the surface of RM4 which supplementary promoted H_2O_2 activation [29]. XPS spectrum of O 1s in Fig. 3c was divided into two peaks. The peak at 530.3 eV belonged to O-metal bond, and the peak of 531.5 eV was corresponded to the adsorbed hydroxyl groups on the surface of RM4. Similar results were found by Wang et al. [11]. The high-resolution XPS spectrum of Fe 2p of RM4 in Fig. 3d presented two obvious peaks. The binding energies at 712.2 and 725.5 eV were ascribed to Fe^{3+} 2p3/2, Fe^{3+} 2p1/2, respectively, which agreed with the results of the report by Wang et al. [30].

According to the characterizations of XRD, SEM and XPS, it could be concluded that a-Fe_2O_3 and b-Fe_2O_3 formed obviously on the surface of RM4. These oxides could promote H_2O_2 activation and then accelerate phenol degradation [20].

3.2. Catalytic activity

In order to investigate the influences of different catalysts on the degradation process of phenol, the removal efficiency of phenol was compared via the catalytic action of RM3, RM4, RM5, RM6, WRM, MFO and FO. As shown in Fig. 4a, RM3, RM4, RM5, RM6 and WRM provided respectively about 7.2%, 96.8%, 80.4%, 16.2% and 17.1% of phenol removal in the catalyst/H_2O_2 system within 120 min. RM4 showed the most efficient catalytic capacity. It could be that a higher content of a-Fe_2O_3 and b-Fe_2O_3 was dispersed on the surface of particles. It was found that 25.22% Al_2O_3, 22.35% SiO_2, 18.46% Fe_2O_3, 8.51% TiO_2, 0.43% NiO, 0.33% MnO, etc were in RM4 by the analysis of XRF. Fe_2O_3 had the higher content in RM4 compared with WRM (described in section 2.1). The catalytic capacity of MFO was far better than FO due to the formation of b-Fe_2O_3 under the acidic condition. Catalytic degradation capacity of RM4 was higher than MFO which was treated under the same

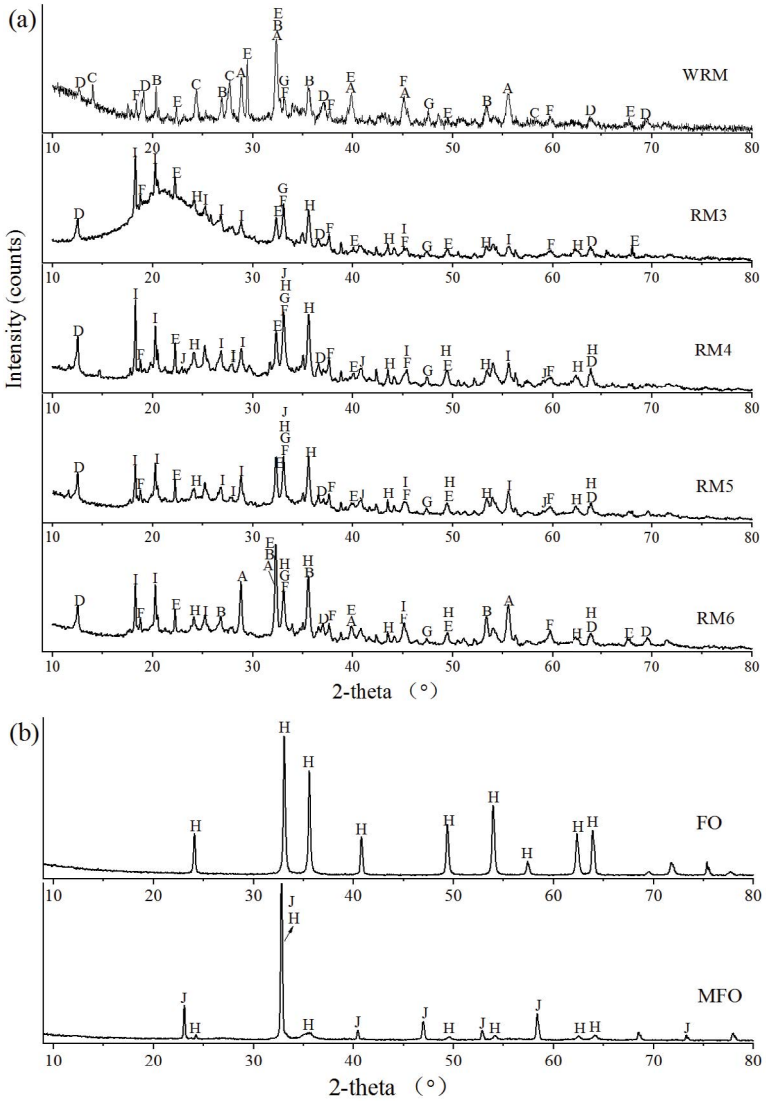

Fig. 1. XRD patterns of WRM, RM3, RM4, RM5, RM6, FO and MFO (A-$Ca_3Al_2(SiO_4)(OH)_8$, B-$Ca_3AlFe(SiO_4)(OH)_8$, C-$Na_8(AlSiO_4)_6(CO_3)(H_2O)_2$, D-$MnO_2$, E-$Ca_2SiO_4$, F-$NiAl_2O_4$, G-$CaTiO_3$, H-$\alpha$-$Fe_2O_3$, I-$Al(OH)_3$, J-$\beta$-$Fe_2O_3$).

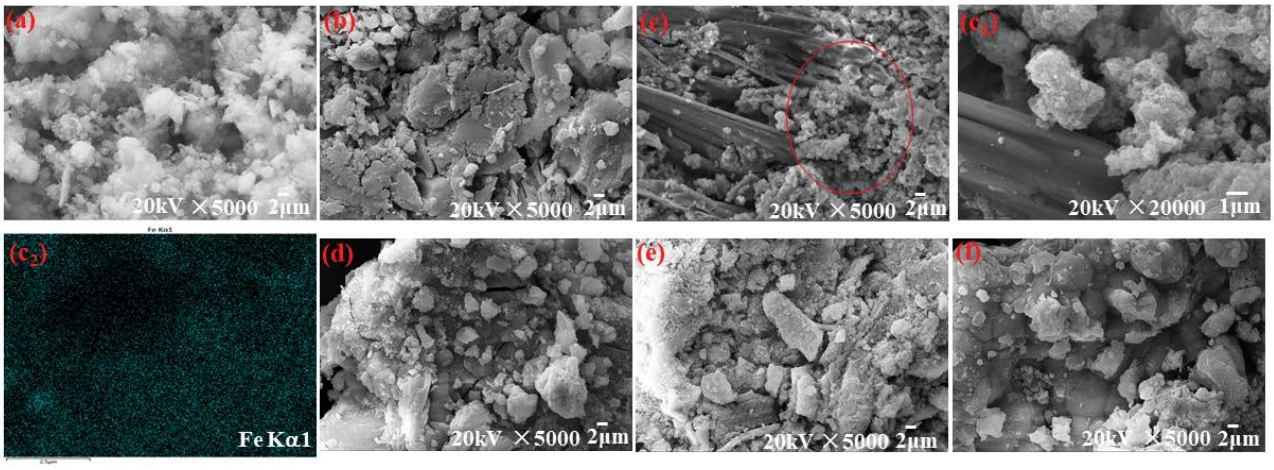

Fig. 2. SEM patterns of WRM (a), RM3 (b), RM4 (c–c_2), RM5 (d), RM6 (e) and MFO (f).

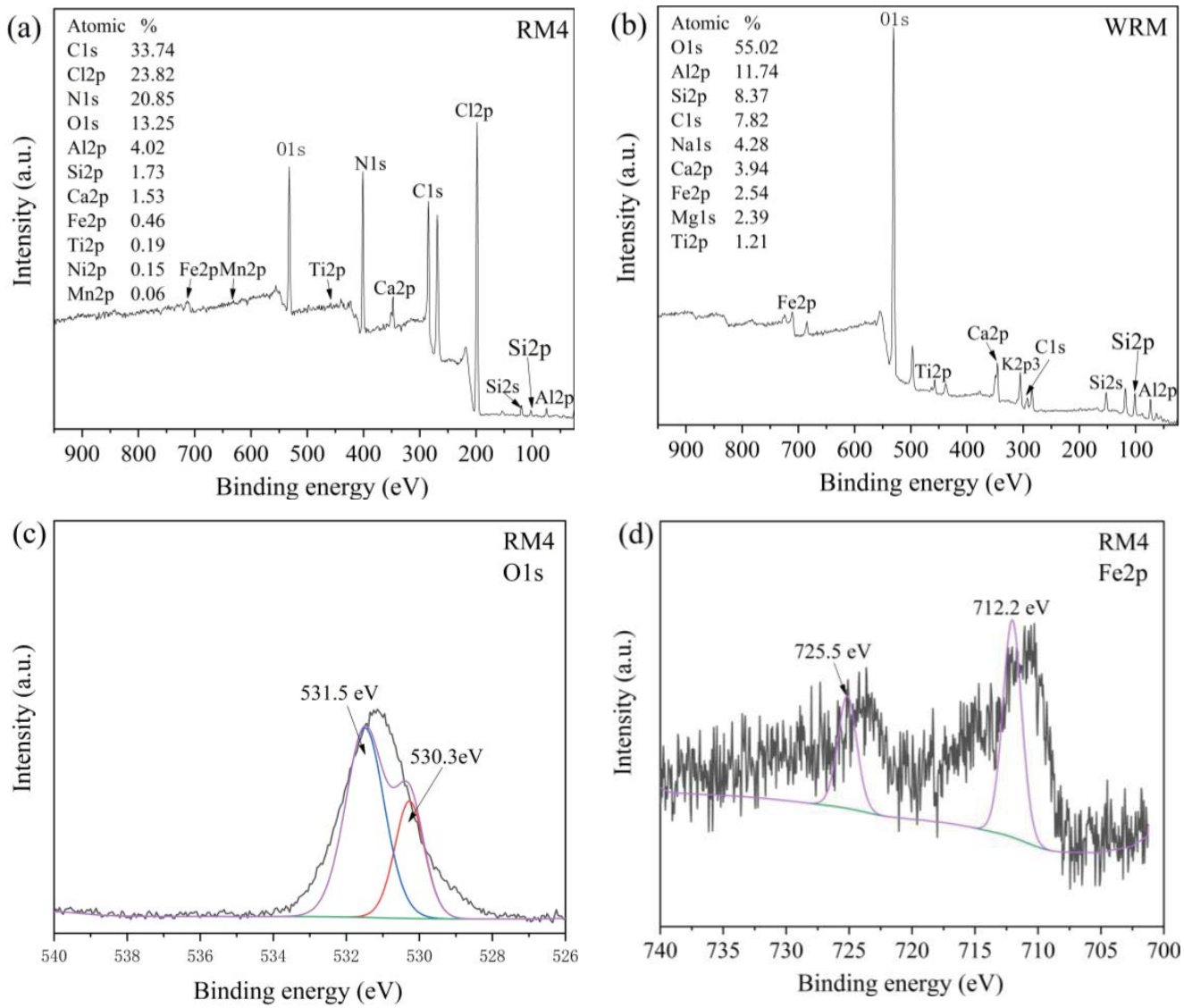

Fig. 3. XPS spectra (the total XPS survey of RM4 (a) and WRM (b), O 1s scan (c) and Fe 2p scan (d) of RM4).

conditions as the RM4 preparation. This suggesting that some trace metal oxides (MnO_2) possibly promoted the catalytic capacity of Fe_2O_3 in RM4 for the phenol degradation [11]. Therefore, the RM4/H_2O_2 system was chosen for the tests of phenol degradation in the following sections. The pH values of solution dropped below 3.5 as for RM4, RM5 and MFO whose catalytic degradation efficiency for phenol were higher than other samples, related to the consumption of H_2O_2 to generate H^+.

The influences of reaction conditions, such as H_2O_2 concentration, initial concentration of phenol, initial pH and catalyst dosage, on the phenol degradation efficiency were investigated, and the results are shown in Fig. 4b and e. The removal efficiency of phenol under different H_2O_2concentration is presented in Fig. 4b. Increasing H_2O_2 concentration from 0 to 0.02 M caused a significant removal efficiency improvement from 0.36% to 96.8%, probably due to more HARs production. However, with further increase of H_2O_2 to 0.1 M, the removal efficiency of phenol had almost no increase, probably ascribed to the quenching impact of excessive H_2O_2 towards HARs [31]. Only 0.36% of phenol removal was observed when RM4 was added into the phenol solution without H_2O_2, which was caused by phenol adsorption on RM4. The pH of point of zero charge (pH_{pzc}) of RM4 was determined by the reported method [32] and the obtained value was 5.74. When solution pH is lower than 5.74, the surface of RM4 could adsorb hydronium ions in solutions. Consequently, the net surface charge of the surfaces of RM4 at pH below the pH_{pzc} is positive after adsorption of hydronium ions. This led to the poor adsorption performance of RM4 under the acidic conditions, which also was confirmed by Fig. 4b. Therefore, the phenol was removed hardly only by the adsorption. 0.02 M of H_2O_2 was selected for the other experiments. The impact of initial concentration of phenol on its degradation is shown in Fig. 4c. The removal efficiency of phenol declined as the initial concentration of phenol increased. The possible cause might be that the excessive

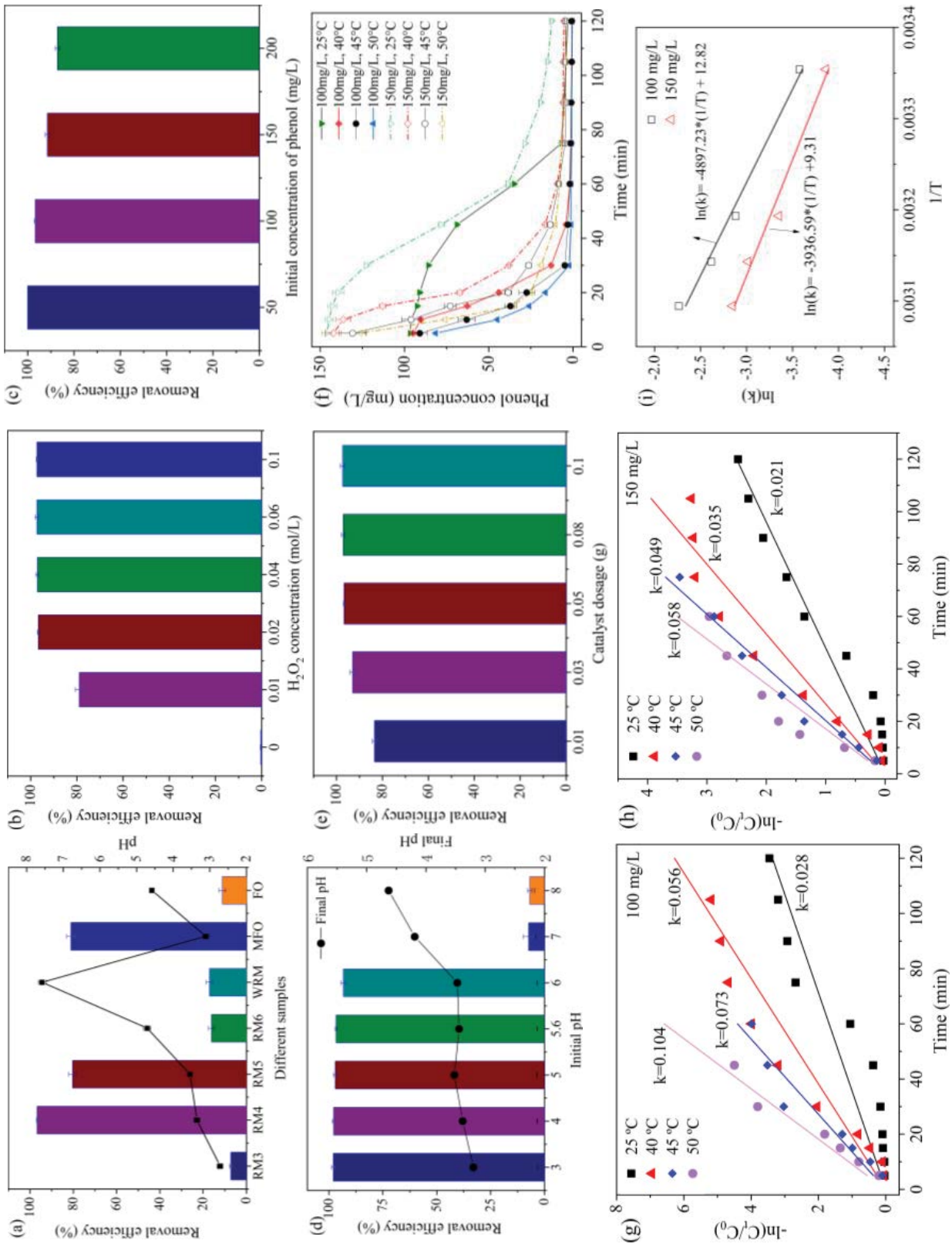

Fig. 4. Phenol degradation by different samples at room temperature (a); influences of the H_2O_2 concentration (b), initial concentration of phenol (c), initial pH (d) and catalyst dosage (e) on the degradation of phenol; The change of phenol degradation with reaction time by RM4 under different temperatures (f); The k values of pseudo-first-order kinetics model of the degradation of 100 or 150 mg/L phenol by RM4 (g and h) and Arrhenius plot of RM4 catalyzing phenol degradation (i).

phenol adsorbed on active sites. The limited active sites for HARs production were responsible for the decreased degradation efficiency [10]. The impact of initial pH on phenol degradation is shown in Fig. 4d with initial pH 3–8. Phenol degradation results were similar between pH 3–6 and had a great increase, suggesting RM4 exhibited pH-independent catalytic activity between pH 3–6. The final pH was <4 after the phenol degradation under different initial pH, probably duo to the production and accumulation of carboxylic intermediates in the process of phenol degradation. However, the removal efficiency was tremendously inhibited when pH exceeded 7. This might be due to deprotonation of H_2O_2 and convert it to less oxidizing •OH [33]. In addition, OH^- under alkaline condition would be adsorbed on the catalyst surface, tend to repulse •OH and slow down the HARs formation [33]. Fig. 4e showed that the phenol removal efficiency was gradually improved with the increase of catalyst dosage, since more active sites were provided for H_2O_2 activation to generate more HARs. However, the increased removal efficiency was little when the added catalyst dosage was greater than 0.05 g. Thus, 0.05 g of RM4 catalyst was selected for the following study. According to the above analysis, the optimized conditions of phenol degradation were 0.02 M H_2O_2, 0.05 g RM4, 120 min of reaction time at 25°C, and had an advantage compared with experiment conditions of relevant studies of phenol degradation (shown in Table 1). The cost of phenol degradation was about $5.58 per ton of phenol solution under the optimized degradation conditions shown in Table 2.

Fig. 4f presents the concentration decrease of 100 and 150 mg/L of phenol with reaction time at different temperatures. The removal efficiency of 100 mg/L phenol was superior to that of 150 mg/L phenol at the same temperature. Inferior degradation capacity of 150 mg/L phenol was ascribed to the relatively insufficient oxidant and the limited active sites. In addition, higher temperature promoted phenol degradation. The removal efficiency of 100 or 150 mg/L of phenol gradually increased as reaction temperature rising from 25°C to 50°C at certain time, indicating that H_2O_2-mediated oxidation of phenol was usually related with the temperature. This was ascribed to the fact that heating promoted H_2O_2 activation [35]. Considering the energy consumption, 25°C was selected as the experiment temperature when the influences of experiment conditions were investigated. As is shown in Fig. 4g and h and Table 3, the degradation reaction of 100 or 150 mg/L of phenol fit into pseudo-first-order kinetics model [Eq. (2)]. the rate constants (k) of 100 mg/L phenol degradation by RM4 at 25°C, 40°C, 45°C and 50°C were 0.028, 0.056, 0.073 and 0.104 min^{-1}, respectively. Likewise, the k values of 25°C, 40°C, 45°C and 50°C for 150 mg/L phenol degradation were 0.021, 0.035, 0.049 and 0.058 min^{-1}, respectively. The rate constants of 100 mg/L phenol degradation outweighed those of 150 mg/L phenol degradation with reference to 25°C, 40°C, 45°C and 50°C, implying the lower concentration of phenol had more excellent removal efficiency.

Fig. 4i shows Arrhenius plots of RM4 catalyzing phenol degradation about 100 and 150 mg/L of phenol. The apparent activation energy (E_a) was calculated from the logarithmic form of Arrhenius equation of the Eq. (3). Where k is the apparent rate constant of phenol degradation, A is the pre-exponential factor, T is the absolute temperature and R is the general gas constant. By calculation, E_a values of 100 and 150 mg/L of phenol were 40.7 and 32.7 kJ/mol, respectively, which were lower than that of other catalysts (48–87 kJ/mol) [5,36]. E_a values were much higher than the diffusion-controlled reaction (10–13 kJ/mol), indicating that the phenol degradation process was mainly controlled by the inherent chemical reaction occurring on the RM4 surface [35]. In addition, The E_a value of 100 mg/L phenol was greater than that of 150 mg/L phenol, indicating the degradation of 100 mg/L phenol had more sensitiveness to temperature.

$$\ln\left(\frac{C_t}{C_0}\right) = kt \tag{2}$$

$$\ln k = -\frac{E_a}{RT} + \ln A \tag{3}$$

To determine the effect of inorganic anions, the removal efficiency of phenol was investigated after adding different concentration of Cl^-, NO_3^- or SO_4^{2-} into the reaction system. Fig. 5a shows that the sequence of the removal efficiency of phenol under Cl^-, NO_3^- and SO_4^{2-} was $Cl^- > NO_3^- > SO_4^{2-}$. However, the difference of removal efficiency of phenol was not tremendous among Cl^-, NO_3^- and SO_4^{2-}. The degradation of phenol was not inhibited evidently by Cl^-, NO_3^- or SO_4^{2-} as the added concentration increased. This signified that the degradation of phenol was not basically attenuated by common ingredients in the simulated wastewater. Fig. 5b presents that the concentration of Fe^{3+} and Na^+ was 6.8 and 38.4 mg/L, respectively, in the RM4/H_2O_2 system after 120 min of reaction time. Therefore, the effect of the RM4/H_2O_2 system on environment was negligible in the degradation process of phenol. Fig. 5c shows that the removal efficiency of COD increased with the reaction time under the optimized degradation conditions. When the removal efficiency of phenol increased to 96.8% within 120 min at 25°C, the removal efficiency of COD reached 88.2% and the value of COD fell to 32 mg/L correspondingly, whose inconsistency signified that carboxylic intermediates probably accumulated in the degradation process. To evaluate the reusability of RM4, the used RM4 was separated by filtration and then carried out naturally air-dried for the next phenol degradation test. The cycle tests (shown in Fig. 5d) indicated that the attenuation of the removal efficiency of phenol increased

Table 2
Economic analysis of phenol degradation under the optimized conditions

Items	Market price	Treated m-cresol solution	
HCl	$2.55/kg	1.7 kg/t	$4.34/t
H_2O_2	$1.20/kg	1.02 kg/t	$1.22/t
NH_3	$0.33/kg	0.06 kg/t	$0.02/t
Total	–	–	$5.58

"–" means that there is no value.

gradually with the increase in cycle number, probably due to the dissolution of iron ions. After four runs, 74.2% removal efficiency of phenol suggested that RM4 possessed an excellent reusability for the phenol degradation in the RM4/H_2O_2 system. The percentage of iron lixiviation was estimated 5.3% in Fe_2O_3 content of the catalyst. After four runs in cycle numbers, the percentage of iron lixiviation reached 23.9%, which was the main cause of the gradual attenuation of phenol removal along with the cycle numbers.

3.3. Mechanism

Quenching experiments were conducted to confirm HARs in the RM4/H_2O_2 system during the degradation of phenol. In general, both methanol and *tert*-butanol could be served as the scavengers of •OH due to their high reaction rate constants with •OH, and the *k* constants were 3.2×10^6 and 7.6×10^8 M/s, respectively [37]. The results, as shown in Fig. 6a, indicated that after addition of methanol or *tert*-butanol, the removal efficiency of phenol in the bulk solution decreased seriously compared with that of

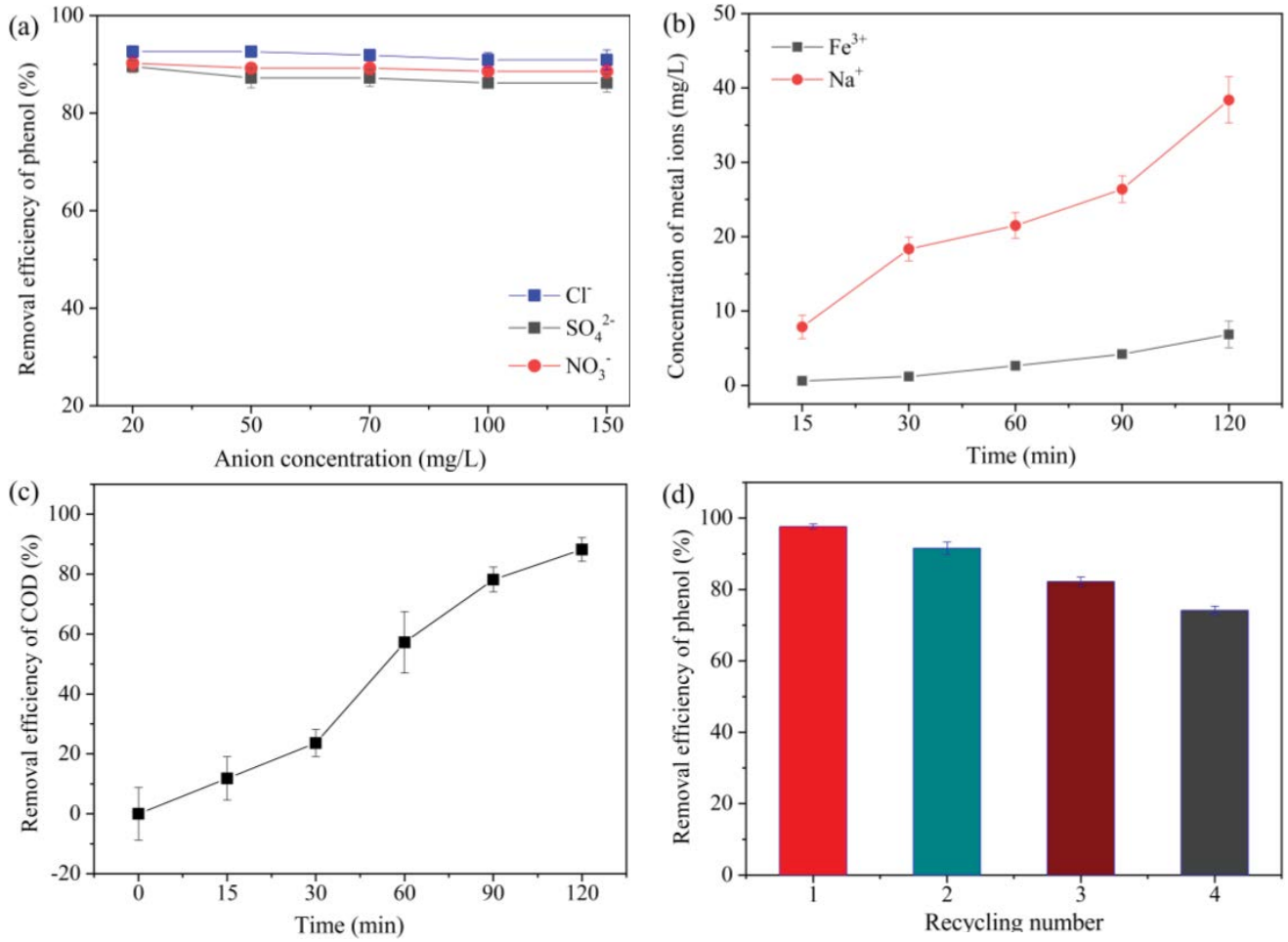

Fig. 5. Influences of different anions on phenol degradation in the RM4/H_2O_2 system (a); the change of concentration of Fe^{3+} and Na^+ ions with reaction time (b); the change of removal efficiency of COD with reaction time (c) and removal efficiency of phenol in cycle tests (d).

Table 3
Correlation coefficients of kinetics model

Concentration (mg/L)	Temperature (°C)	R^2	Concentration (mg/L)	Temperature (°C)	R^2
100	25	0.9863	150	25	0.9907
	40	0.9901		40	0.9861
	45	0.9782		45	0.9983
	50	0.9870		50	0.9694
	Arrhenius equation	0.9805		Arrhenius equation	0.9698

the same conditions without the scavengers, which meant that •OH played the dominant role in the RM4/H_2O_2 system. ESR experiments were also executed using DMPO as a •OH spin-trapping probe. The quartet peaks with an intensity ratio of 1:2:2:1 were the signals of DMPO-OH adduct (observed in Fig. 6b). This result further confirmed the existence of •OH in the RM4/H_2O_2 system. On the contrary, there were not the signals of DMPO-OH adduct in the system without the catalyst. Thus, •OH was generated during H_2O_2 activation by RM4. The possible degradation mechanism was proposed as follows: The surface bonded $^{\equiv}Fe^{3+}$ species (a-Fe_2O_3 and b-Fe_2O_3) reacted with the adsorbed H_2O_2 and HOO• generated by Eq. (4) to form $^{\equiv}Fe^{2+}$ [Eqs. (4) and (5)] [38]. $^{\equiv}Fe^{2+}$ would activate H_2O_2 to generate •OH by Eq. (6). During the reaction, a bit of $^{\equiv}Mn^{4+}$ species (MnO_2) of RM4 was reduced to$^{\equiv}Mn^{3+}$ by H_2O_2 [Eq. (7)] [39]. In addition, $^{\equiv}Mn^{3+}$ prompted $^{\equiv}Fe^{3+}$ to convert to $^{\equiv}Fe^{2+}$ [Eq. (8)] [31], which was why the catalytic capacity of RM4 for phenol degradation was higher than MFO. Then the produced •OH rapidly attacked the phenol to generate intermediates and further mineralized them into CO_2 and H_2O [Eq. (9)]. The intermediates were analyzed by using LCMS during the degradation of phenol in the RM4/H_2O_2 system, as shown in Table 4. The possible intermediates mainly included 1,2-benzenediol, benzoquinone, muconic acid, maleic acid, oxalic acid, acetic acid, etc. Fig. 7 illustrated a possible reaction process and mechanism during the degradation of phenol in the RM4/H_2O_2 system.

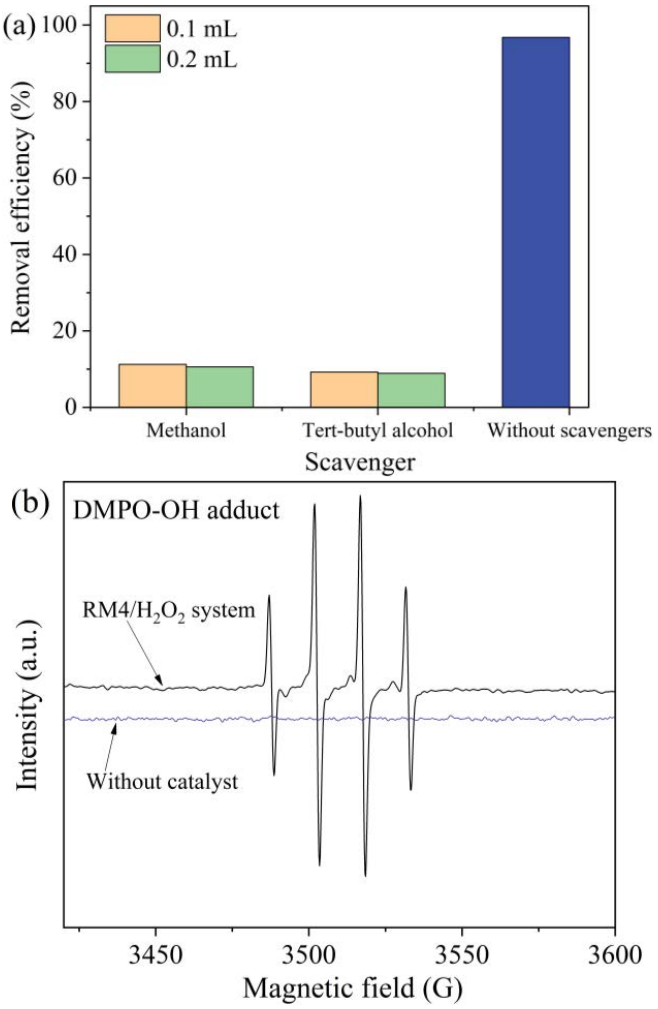

Fig. 6. Influences of methanol and *tert*-butanol on the phenol degradation (a) and DMPO-OH adduct of trapping •OH (b).

$$\equiv Fe^{3+} + H_2O_2 \rightarrow \equiv Fe^{2+} + HOO + H^+ \quad (4)$$

$$\equiv Fe^{3+} + HOO \rightarrow \equiv Fe^{2+} + O_2 + H^+ \quad (5)$$

$$\equiv Fe^{2+} + H_2O_2 \rightarrow \equiv Fe^{3+} + OH + OH^- \quad (6)$$

$$\equiv Mn^{4+} + H_2O_2 \rightarrow \equiv Mn^{3+} + HOO + H^+ \quad (7)$$

$$\equiv Mn^{3+} + \equiv Fe^{3+} \rightarrow \equiv Mn^{4+} + Fe^{2+} \quad (8)$$

$$C_6H_6 + OH \rightarrow \text{intermediates} \rightarrow CO_2 + H_2O \quad (9)$$

3.4. Continuous phenol degradation

Continuous experiments were carried out using RM4 catalyst with the best catalytic performance via a self-made device (Fig. 8a). The synthetic solutions of phenol with 50–200 mg/L under different flows (0.2–2.5 mL/min) were applied to such experiments. The dosage of catalyst loading in the column was 2 g and the range of residence time

Table 4
Possible intermediates by LCMS during the phenol degradation in the RM4/H_2O_2 system

No.	m/z	Molecular formula	Chemical name
1	110	$C_6H_6O_2$	1,2-Benzenediol
2	94	C_6H_6O	Phenol
3	108	$C_6H_4O_2$	Benzoquinone
4	142	$C_6H_4O_4$	Muconic acid
5	115	$C_4H_4O_4$	Maleic acid
6	90	$C_2H_2O_4$	Oxalic acid
7	60	$C_2H_4O_2$	Acetic acid

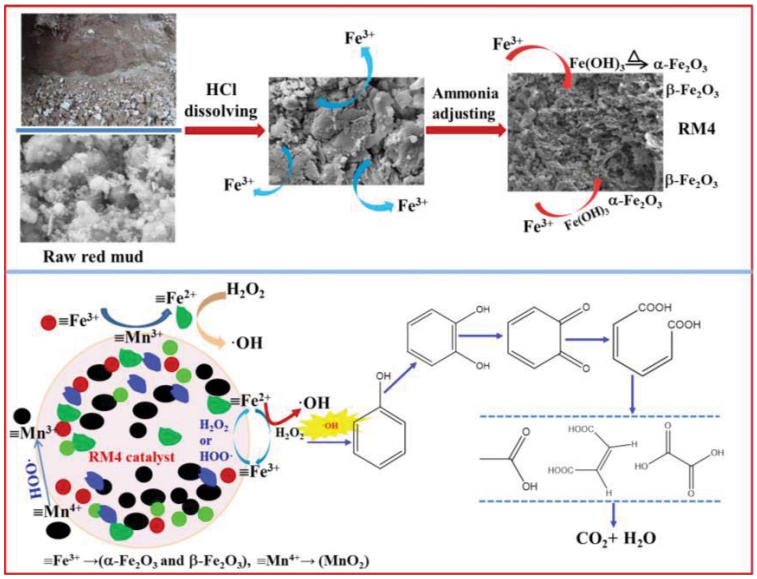

Fig. 7. Schematic diagrams of the change of Fe components during RM4 preparation and the mechanism of phenol degradation by RM4.

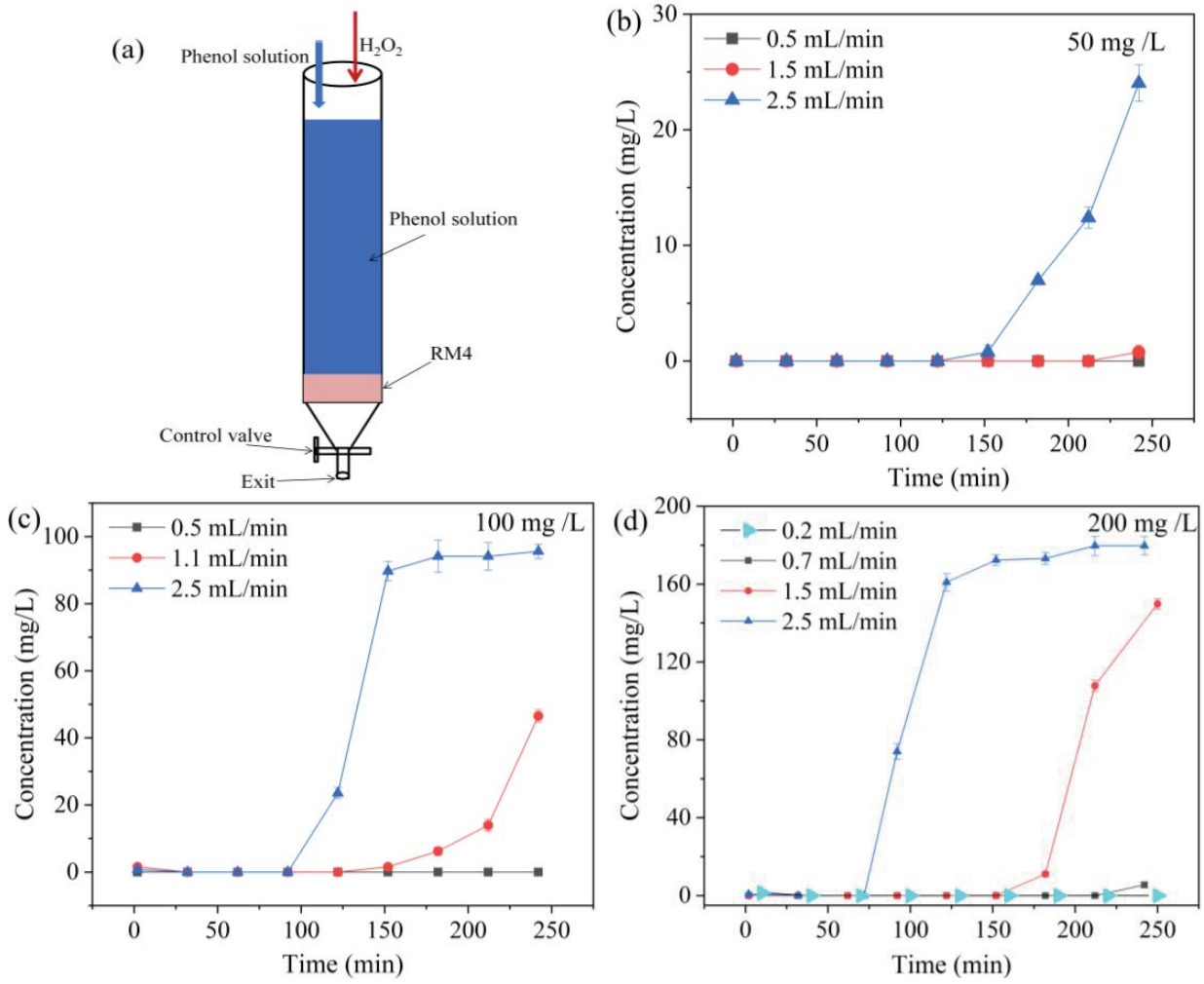

Fig. 8. Results of continuous experiments of phenol degradation.

was about 17–215 min consistent with 0.2–2.5 mL/min of flows. The phenol concentration of solution from the exit of the experiment setup was analyzed at expected time. Fig. 8b–d shows that the greater the flow was, the earlier the high concentration of phenol came as for different concentration of phenol. As for 50 mg/L of phenol, when the flow was lower than 1.5 mL/min, the phenol was thoroughly removed during experiments. The concentration of phenol increased significantly since 150 min at 2.5 mL/min of the flow. The concentration of phenol increased significantly from 150 min as the flow was 1.1 mL/min for 100 mg/L of phenol. The high concentration of phenol arrived earlier at 2.5 mL/min of the flow. The degradation effect of phenol was poorer for 200 mg/L of phenol when the flow exceeded 1.5 mL/min. These finding indicated the low concentration of phenol was easily degraded by H_2O_2 using the RM4 catalyst under a relative low flow. The results indicated that phenol could be removed via continuous experiments in the column and offered a reference for further pilot scale tests.

4. Conclusions

Phenol is universally recognized as the most toxic, widely distributed and serious health hazard component among various phenolic pollutants. RM, a solid waste generated during the bauxite refining of alumina, contains plenty of SiO_2, Al_2O_3, CaO, Fe_2O_3, TiO_2, and a small quantity of MnO, ZrO_2, SrO, NiO, NbO, etc and has the potential of catalyzing phenol degradation.

In this study, a novel and inexpensive acid-modified RM containing abundant functional groups (α-Fe_2O_3, β-Fe_2O_3) and pore structures was prepared. RM4 activating H_2O_2 process was firstly applied to the degradation of phenol. 96.8% of the phenol degradation was achieved within 120 min under the conditions of 0.02 M of H_2O_2, 100 mg/L of phenol, 0.05 g of RM4. In addition, RM4 exhibited the pH-independent catalytic activity within pH 3–6. The degradation reaction of 100 and 150 mg/L of phenol fit into pseudo-first-order kinetics model at 25°C–50°C under the optimum conditions. E_a value of 100 mg/L phenol was greater than that of 150 mg/L phenol, indicating the degradation of 100 mg/L phenol had more sensitiveness to temperature. The degradation of phenol was not inhibited evidently by Cl^-, NO_3^- or SO_4^{2-} as the added concentration increased. When the removal efficiency of phenol increased to 96.8%, the removal efficiency of COD reached 88.2%, whose inconsistency signified that carboxylic intermediates probably accumulated in the degradation process.

Quenching and ESR experiments confirmed that $^{\bullet}OH$ was the predominant radical and responsible for the formation of DMPO-OH adduct. α-Fe_2O_3 and β-Fe_2O_3 in RM4 played crucial roles in the H_2O_2 activation for $^{\bullet}OH$ production. The results of the continuous experiments offered a reference to further pilot scale tests.

Acknowledgments

This work was financially supported by the National Natural Science Foundation of China (No. 21868001) and the Guizhou Science and Technology Department (No. Qiankehejichu [2019]1040).

Author contribution

Hongliang Chen: Methodology, Formal analysis, Funding acquisition, Software, Data curation, Writing-original draft, Writing-review and editing; Qian Long: Conceptualization, Formal analysis, Visualization; Fuhua Wei: Conceptualization, Supervision, Project administration, Investigation.

Conflicts of interest

The authors declare no conflicts of interest.

References

[1] H. Li, R. Cheng, Z. Liu, C. Du, Waste control by waste: Fenton–like oxidation of phenol over Cu modified ZSM–5 from coal gangue, Sci. Total Environ., 683 (2019) 638–647.
[2] A. Dargahi, H.R. Barzoki, M. Vosoughi, S. Ahmad Mokhtari, Enhanced electrocatalytic degradation of 2,4-Dinitrophenol (2,4-DNP) in three-dimensional sono-electrochemical (3D/SEC) process equipped with Fe/SBA-15 nanocomposite particle electrodes: degradation pathway and application for real wastewater, Arabian J. Chem., 15 (2022) 103801, doi: 10.1016/j.arabjc.2022.103801.
[3] E. Brillas, S. Garcia-Segura, Benchmarking recent advances and innovative technology approaches of Fenton, photo-Fenton, electro-Fenton, and related processes: a review on the relevance of phenol as model molecule, Sep. Purif. Technol., 237 (2020) 116337, doi: 10.1016/j.seppur.2019.116337.
[4] P.J. Ong, A. Priyadarshini, S.W. Tay, L. Hong, Affinity filtration by a coating of pyrolyzed fish scale colloids on microfibres for removing phenol/quinone compounds from alcohols, J. Environ. Chem. Eng., 9 (2021) 106097, doi: 10.1016/j.jece.2021.106097.
[5] A. Dargahi, M.R. Samarghandi, A. Shabanloo, M.M. Mahmoudi, H.Z. Nasab, Statistical modeling of phenolic compounds adsorption onto low-cost adsorbent prepared from aloe vera leaves wastes using CCD-RSM optimization: effect of parameters, isotherm, and kinetic studies, Biomass Convers. Biorefin., (2021) 1–15, doi: 10.1007/s13399-021-01601-y.
[6] A. Almasi, M. Mahmoudi, M. Mohammadi, A. Dargahi, H. Biglari, Optimizing biological treatment of petroleum industry wastewater in a facultative stabilization pond for simultaneous removal of carbon and phenol, Toxin Rev., 40 (2019) 189–197.
[7] R. Shokoohi, H. Movahedian, A. Dargahi, A.J. Jafari, A. Parvaresh, Survey on efficiency of BF/AS integrated biological system in phenol removal of wastewater, Desal. Water Treat., 82 (2017) 315–321.
[8] P. Gao, Y. Song, M. Hao, A. Zhu, H. Yang, S. Yang, An effective and magnetic Fe_2O_3-ZrO_2 catalyst for phenol degradation under neutral pH in the heterogeneous Fenton-like reaction, Sep. Purif. Technol., 201 (2018) 238–243.
[9] R. Sun, J. Yang, R. Huang, C. Wang, Controlled carbonization of microplastics loaded nano zero-valent iron for catalytic degradation of tetracycline, Chemosphere, 3030 (2022) 135123, doi: 10.1016/j.chemosphere.2022.135123.
[10] J. Gao, Y. Liu, X. Xia, L. Wang, W. Dong, $Fe_{1-x}Zn_xS$ ternary solid solution as an efficient Fenton-like catalyst for ultrafast degradation of phenol, J. Hazard. Mater., 353 (2018) 393–400.
[11] J. Wang, T. Xie, G. Han, Q. Zhu, Y. Wang, Y. Peng, S. Liu, Z. Yao, SiO_2 mediated templating synthesis of γ-Fe_2O_3/MnO_2 as peroxymonosulfate activator for enhanced phenol degradation dominated by singlet oxygen, Appl. Surf. Sci., 560 (2021) 149984, doi: 10.1016/j.apsusc.2021.149984.
[12] J. Zhang, S. Zhang, B. Liu, Degradation technologies and mechanisms of dioxins in municipal solid waste incineration fly ash: a review, J. Cleaner Prod., 250 (2020) 119507, doi: 10.1016/j.jclepro.2019.119507.
[13] C. Shi, X. Wang, S. Zhou, X. Zuo, C. Wang, Mechanism, application, influencing factors and environmental benefit

assessment of steel slag in removing pollutants from water: a review, J. Water Process Eng., 47 (2022) 102666, doi: 10.1016/j.jwpe.2022.102666.
[14] J. Lan, Y. Sun, P. Huang, Y. Du, W. Zhan, T.C. Zhang, D. Du, Using electrolytic manganese residue to prepare novel nanocomposite catalysts for efficient degradation of azo dyes in Fenton-like processes, Chemosphere, 252 (2020) 126487, doi: 10.1016/j.chemosphere.2020.126487.
[15] N. Nasuha, B.H. Hameed, P.U. Okoye, Dark-Fenton oxidative degradation of methylene blue and acid blue 29 dyes using sulfuric acid-activated slag of the steel-making process, J. Environ. Chem. Eng., 9 (2021) 104831, doi: 10.1016/j.jece.2020.104831.
[16] Y. Xu, E. Hu, D. Xu, Q. Guo, Activation of peroxymonosulfate by bimetallic CoMn oxides loaded on coal fly ash-derived SBA-15 for efficient degradation of Rhodamine B, Sep. Purif. Technol., 274 (2021) 119081, doi: 10.1016/j.seppur.2021.119081.
[17] B. Qiu, C. Yang, Q. Shao, Y. Liu, H. Chu, Recent advances on industrial solid waste catalysts for improving the quality of bio-oil from biomass catalytic cracking: a review, Fuel, 315 (2022) 123218, doi: 10.1016/j.fuel.2022.123218.
[18] J. Wang, S. Zhang, D. Xu, H. Zhang, Catalytic activity evaluation and deactivation progress of red mud/carbonaceous catalyst for efficient biomass gasification tar cracking, Fuel, 323 (2022) 124278, doi: 10.1016/j.fuel.2022.124278.
[19] B. Das, K. Mohanty, A review on advances in sustainable energy production through various catalytic processes by using catalysts derived from waste red mud, Renewable Energy, 143 (2019) 1791–1811.
[20] M. Wang, X. Liu, Applications of red mud as an environmental remediation material: a review, J. Hazard. Mater., 408 (2021) 124420, doi: 10.1016/j.jhazmat.2020.124420.
[21] C. Wang, X. Zhang, R. Sun, Y. Cao, Neutralization of red mud using bio-acid generated by hydrothermal carbonization of waste biomass for potential soil application, J. Cleaner Prod., 271 (2020) 122525, doi: 10.1016/j.jclepro.2020.122525.
[22] L. Wang, B. Si, X. Han, W. Yi, Z. Li, A. Zhang, Study on the effect of red mud and its component oxides on the composition of bio-oil derived from corn stover catalytic pyrolysis, Ind. Crops Prod., 184 (2022) 114973, doi: 10.1016/j.indcrop.2022.114973.
[23] S. Agrawal, N. Dhawan, Evaluation of red mud as a polymetallic source – a review, Miner. Eng., 171 (2021) 107084, doi: 10.1016/j.mineng.2021.107084.
[24] J. Ba, G. Wei, L. Zhang, Q. Li, Z. Li, J. Chen, Preparation and application of a new Fenton-like catalyst from red mud for degradation of sulfamethoxazole, Environ. Technol., 43 (2022) 2922–2933.
[25] R. Sun, X. Zhang, C. Wang, Y. Cao, Co-carbonization of red mud and waste sawdust for functional application as Fenton catalyst: evaluation of catalytic activity and mechanism, J. Environ. Chem. Eng., 9 (2021) 105368, doi: 10.1016/j.jece.2021.105368.
[26] L. Yu, Y. Liu, H. Wei, L. Chen, L. An, Developing a high-quality catalyst from the pyrolysis of anaerobic granular sludge: its application for m-cresol degradation, Chemosphere, 255 (2020) 126939, doi: 10.1016/j.chemosphere.2020.126939.
[27] H. Habibi, D. Piruzian, S. Shakibania, Z. Pourkarimi, M. Mokmeli, The effect of carbothermal reduction on the physical and chemical separation of the red mud components, Miner. Eng., 173 (2021) 107216, doi: 10.1016/j.mineng.2021.107216.
[28] Y. Zhang, N. Zhang, T. Wang, H. Huang, Y. Chen, Z. Li, Z. Zou, Heterogeneous degradation of organic contaminants in the photo-Fenton reaction employing pure cubic β-Fe_2O_3, Appl. Catal., B, 245 (2019) 410–419.
[29] N.A. Fathy, S.E. El-Shafey, O.I. El-Shafey, W.S. Mohamed, Oxidative degradation of RB19 dye by a novel γ-MnO_2/MWCNT nanocomposite catalyst with H_2O_2, J. Environ. Chem. Eng., 1 (2013) 858–864.
[30] C. Wang, R. Sun, R. Huang, Highly dispersed iron-doped biochar derived from sawdust for Fenton-like degradation of toxic dyes, J. Cleaner Prod., 297 (2021) 126681, doi: 10.1016/j.jclepro.2021.126681.
[31] B. Li, Z.-Y. Yan, X.-N. Liu, C. Tang, J. Zhou, X.-Y. Wu, P. Wei, H.-H. Jia, X.-Y. Yong, Enhanced bio-electro-Fenton degradation of phenolic compounds based on a novel Fe–Mn/graphite felt composite cathode, Chemosphere, 234 (2019) 260–268.
[32] N. Omrani, A. Nezamzadeh-Ejhieh, Focus on scavengers' effects and GC-MASS analysis of photodegradation intermediates of sulfasalazine by Cu_2O/CdS nanocomposite, Sep. Purif. Technol., 235 (2020) 116228, doi: 10.1016/j.seppur.2019.116228.
[33] X. Xu, Y. Feng, Z. Chen, S. Wang, G. Wu, T. Huang, J. Ma, G. Wen, Activation of peroxymonosulfate by $CuCo_2O_4$-GO for efficient degradation of bisphenol A from aqueous environment, Sep. Purif. Technol., 251 (2020) 117351, doi: 10.1016/j.seppur.2020.117351.
[34] E. Saputra, S. Muhammad, H. Sun, H.M. Ang, M.O. Tadé, S. Wang, Red mud and fly ash supported Co catalysts for phenol oxidation, Catal. Today, 190 (2012) 68–72.
[35] B. Liu, W. Song, H. Wu, Y. Xu, Y. Sun, Y. Yu, H. Zheng, S. Wan, Enhanced oxidative degradation of norfloxacin using peroxymonosulfate activated by oily sludge carbon-based nanoparticles $CoFe_2O_4$/OSC, Chem. Eng. J., 400 (2020) 125947, doi: 10.1016/j.cej.2020.125947.
[36] C. Wang, R. Huang, R. Sun, J. Yang, D.D. Dionysiou, Microplastics separation and subsequent carbonization: synthesis, characterization, and catalytic performance of iron/carbon nanocomposite, J. Cleaner Prod., 330 (2022) 129901, doi: 10.1016/j.jclepro.2021.129901.
[37] T. Zhang, Q. Ma, M. Zhou, C. Li, J. Sun, W. Shi, S. Ai, Degradation of methylene blue by a heterogeneous Fenton reaction catalyzed by $FeCo_2O_4$-NC nanocomposites derived by ZIFs, Powder Technol., 383 (2021) 212–219.
[38] H. Wang, M. Jing, Y. Wu, W. Chen, Y. Ran, Effective degradation of phenol via Fenton reaction over CuNiFe layered double hydroxides, J. Hazard. Mater., 353 (2018) 53–61.
[39] W. Shaheen, K. Hong, Thermal characterization and physicochemical properties of Fe_2O_3–Mn_2O_3/Al_2O_3 system, Thermochim. Acta, 381 (2002) 153–164.